PHYSICAL REVIEW E **71**, 020702(R) (2005)

Real-time microbe detection based on director distortions around growing immune complexes in lyotropic chromonic liquid crystals

S. V. Shiyanovskii,[1,2] T. Schneider,[1] I. I. Smalyukh,[1] T. Ishikawa,[1] G. D. Niehaus,[4] K. J. Doane,[5] C. J. Woolverton,[3] and O. D. Lavrentovich[1,2,*]

[1]*Liquid Crystal Institute, Kent State University, Kent, Ohio, 44242, USA*

[2]*Chemical Physics Interdisciplinary Program, Kent State University, Kent, Ohio, 44242, USA*

[3]*Department of Biological Sciences, Kent State University, Kent, Ohio, 44242, USA*

[4]*Department of Physiology, College of Medicine, Northeastern Ohio Universities, Rootstown, Ohio 44272, USA*

[5]*Department of Anatomy, College of Medicine, Northeastern Ohio Universities, Rootstown, Ohio 44272, USA*

(Received 26 May 2004; published 18 February 2005)

We describe director distortions in the nematic liquid crystal (LC) caused by a spherical particle with tangential surface orientation of the director and show that light transmittance through the distorted region is a steep function of the particle's size. The effect allows us to propose a real-time microbial sensor based on a nontoxic lyotropic chromonic LC (LCLC) that detects and amplifies the presence of immune complexes. A cassette is filled with LCLC, antibody, and antigen-bearing particles. Small and isolated particles cause no macroscopic distortions of the LCLC. Upon antibody-antigen binding, the growing immune complexes distort the director and cause detectable optical transmittance between crossed polarizers.

DOI: 10.1103/PhysRevE.71.020702 PACS number(s): 61.30.−v, 42.70.Df, 77.84.Nh, 87.80.−y

There is a growing interest in using liquid crystals (LCs) in biological sensors [1–5]. Abbott *et al.* proposed a technique based on the anchoring the transition at the nematic surface [1]. The LC is aligned in the cell with substrates coated with gold films and surface-bound antigens (ligands). If there is an antibody in the system that binds to the ligands at the surface, the LC director $\hat{\mathbf{n}}$ might change its orientation at the surface and thus in the bulk. Director changes thus detect the antibody-antigen binding. There are three areas for improvement. (1) Alignment of LC at the substrates with receptors is challenging [4], as the receptors should function simultaneously as the antibody-specific sites and as aligning agents for the LC. (2) The LCs capable of anchoring transitions are thermotropic (solvent-free) and oil-like [6], practically immiscible with water, which is the typical carrier of biological species. (3) The thermotropic LCs are often toxic [7,8]. The standard lyotropic LCs formed by amphiphilic (surfactant) molecules [6] are hard to use, because the surfactants (a) alter the integrity of the antigen-presenting cellular membranes, and (b) prefer to align perpendicularly to interfaces making the anchoring transitions difficult to induce.

We describe a physical background of a different sensor, Fig. 1, suitable for real-time detection of microbes in which (1) the director distortions occur in the LC *bulk* triggered by antibody-antigen binding and formation of an immune complex; (2) we use lyotropic chromonic LCs (LCLCs) that are water-based but nonsurfactant [9] and nontoxic [8]; (3) surface alignment of LCLC is achieved in a standard fashion, say, by rubbed polyimide films [10]. The LCLCs are composed of planklike molecules with a polyaromatic central core and hydrophilic ionic (or hydrogen-bonding) groups at the periphery. The basic building block of LCLCs is a molecular stack in which the molecules are arranged face-to-face with ionic groups at the water-aggregate interface [9].

Each microbe has characteristic molecular groups-antigens at the surface, to which the corresponding antibody can bind, thus "recognizing" and "detecting" it [11]. The problem is to amplify this highly selective binding. We propose to use the LCLC medium with the dissolved antibody that targets the microbe of interest, say, anthrax. When the microbes are present, the antigen-antibody binding causes their aggregation into the immune complexes (each antibody molecule has two binding sites) [11] that grow in the LCLC bulk. Physically, an increase in the size d of the foreign inclusion should trigger director distortions once d exceeds some critical size $d_c \sim K/W$ because the elastic energy around the inclusion scales as Kd and the surface anchoring energy scales as Wd^2 [6]. Here K is the Frank elastic constant in a one-constant approximation, and W is the polar anchoring coefficient at the LC particle interface. The cases $d < d_c$ ($\hat{\mathbf{n}} = \text{const}$) and $d > d_c$ [$(\hat{\mathbf{n}} = \hat{\mathbf{n}}(\mathbf{r})$] can be made optically distinct by placing the sample between two crossed polarizers. The intensity of light transmitted through the distorted region around a complex of size $d > d_c$ depends on the details of the director pattern $\hat{\mathbf{n}}(\mathbf{r})$. So far, $\hat{\mathbf{n}}(\mathbf{r})$ has been calculated only for the case when $\hat{\mathbf{n}}$ is perpendicular to the particle surface [12–14]. Our case is different as LCLCs prefer tangential orientation at most surfaces. The associated optical effects have never been calculated before; the problem is challenging as the geometry might imply twist deformations and waveguiding regimes. We find the solutions below and demonstrate that the increase in d does indeed cause a substantial light transmittance around a sufficiently large inclusions.

THEORY

Structure

Consider a sphere of radius R in the nematic slab of thickness $h \gg R$. The cell plates set a unidirectional planar align-

*Electronic address: odl@lci.kent.edu

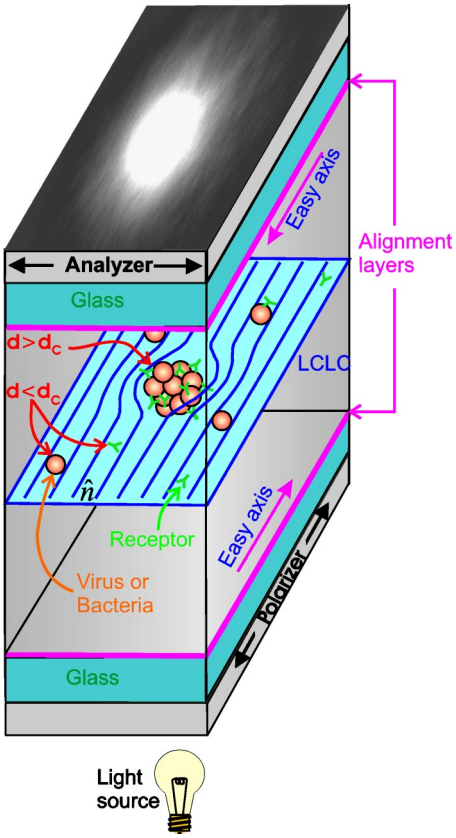

FIG. 1. (Color online) The scheme of the LCLC biosensor for the detection of immune complexes.

ment. In the axial symmetry approximation, director around the particle depends only on the angle $\beta(r,\theta)$ between $\hat{\mathbf{n}}$ and the alignment direction $\hat{\mathbf{a}}$ at the bounding plates, and writes in the spherical coordinates $\{r,\theta,\varphi\}$ as $\hat{\mathbf{n}}=\{\cos(\beta+\theta), -\sin(\beta+\theta),0\}$. The equilibrium $\hat{\mathbf{n}}$ is found by minimizing the sum of the elastic energy and the Rapini-Papoular anchoring term [6]

$$F_{tot}=\frac{K}{2}\int\left[\left(\frac{\partial\beta}{\partial r}\right)^2+\left(\frac{1}{r}\frac{\partial\beta}{\partial\theta}\right)^2+\left(\frac{\sin\beta}{r\sin\theta}\right)^2\right]dV + \frac{1}{2}\int\left[W\cos^2(\beta+\theta)+\frac{K-2K_{24}}{R}\times\left(\frac{\sin\beta}{\sin\theta}\cos(\beta+\theta)+\frac{\partial\beta}{\partial\theta}\right)\right]dS, \quad (1)$$

where K_{24} is the saddle-splay constant, from the equation

$$\nabla^2\beta-\frac{\sin 2\beta}{2r^2\sin\theta}=0. \quad (2)$$

For weak anchoring $R<\xi$, where $\xi=2(K+K_{24})/W$, one can use the linearized solution [12]

$$\beta=\beta_0\left(\frac{R}{r}\right)^3\sin 2\theta, \quad (3)$$

where $\beta_0=R/2[\xi+(R/7)]$.

For $R>\xi$, we use the ansatz

$$\beta=\arctan\frac{g(r)\sin 2\theta}{1+g(r)\cos 2\theta}, \quad (4)$$

which satisfies boundary conditions for both weak $g(R)=\beta_0\ll 1$ and strong $g(R)=1$ anchoring. Equation (3) is a good approximation even for $R>\xi$, with β_0 being a constant.

Optics

We use the Cartesian coordinates $\{x,y,z\}$ with the origin at the particle center; the z axis is normal to the substrates, and the x axis is along $\hat{\mathbf{a}}$, so that

$$\hat{\mathbf{n}}=\left\{\cos\beta,\frac{-y}{\sqrt{y^2+z^2}}\sin\beta,\frac{-z}{\sqrt{y^2+z^2}}\sin\beta\right\}.$$

The polar distortions $\tilde{}n_z$ do not rotate the polarization and cause only a negligible change of the effective extraordinary index; thus we assume that $\hat{\mathbf{n}}$ is confined to the Oxy plane: $\hat{\mathbf{n}}=\{\cos\Theta,\sin\Theta,0\}$, where the rotation angle Θ is derived from Eq. (3)

$$\Theta\cong\frac{-y}{\sqrt{y^2+z^2}}\beta=\frac{-\beta_0\rho^2R^3\sin 2\Phi}{(\rho^2+z^2)^{5/2}}, \quad (5)$$

$\rho=\sqrt{x^2+y^2}$, and $\Phi=\tan^{-1}(y/x)$.

When rotation of $\hat{\mathbf{n}}$ around the z axis is slow, one can describe the light propagation with ordinary and extraordinary waves in a rotating frame $O\xi\eta z$ ($\hat{\mathbf{e}}_\eta\perp\hat{\mathbf{n}}$) and consider the wave transformation as a perturbation caused by the frame rotation with a perturbative parameter $\mu=L\Theta'$, where $L=\lambda(2\pi\Delta n)$ is the retardation length, $\Delta n=n_e-n_o$ is birefringence, λ is the wavelength in vacuum, and prime means the z derivative [15,16]. We use a more advanced approach, taking the exact solutions of the wave equation for a helical structure with a homogeneous rotation $\Theta'=\text{const}$ as the nonperturbed solutions. In the rotating frame $O\xi\eta z$ such a solution for the forward waves reads

$$\tilde{\mathbf{E}}=A_1(\cos\alpha_1\hat{\mathbf{e}}_\xi+i\sin\alpha_1\hat{\mathbf{e}}_\eta)\exp\{i\Psi_1\} + A_2(i\sin\alpha_2\hat{\mathbf{e}}_\xi+\cos\alpha_2\hat{\mathbf{e}}_\eta)\exp\{i\Psi_2\}, \quad (6)$$

where $\Psi_j(z)=\int_{z_0}^{z}q_j d\tilde{z}$ is the phase of the jth wave with the wave vector q_j and the ellipticity α_j that depends on Θ', and z_0 is the coordinate of the input boundary of the LC layer. The inhomogeneity of rotation is a perturbation that affects the amplitudes A_j. Assuming that the rotation inhomogeneity is smooth, $|\Theta'|\lambda<1$, one can neglect the coupling between forward and backward waves. By substituting Eq. (6) in Maxwell equations we derive the following equations using MATHEMATICA 5.0:

$$\cos(\alpha_1-\alpha_2)A_1'=\sin(\alpha_1-\alpha_2)\alpha_1'A_1-i\exp\{-i\Delta\Psi(z)\}\alpha_2'A_2$$

$$\cos(\alpha_1-\alpha_2)A_2'=\sin(\alpha_2-\alpha_1)\alpha_2'A_2-i\exp\{i\Delta\Psi(z)\}\alpha_1'A_1, \quad (7)$$

where $\Delta\Psi(z)=\Psi_1(z)-\Psi_2(z)$ is the phase retardation between the two waves. The birefringence of LCLCs is small: $\delta=\Delta n/(n_e+n_o)=-0.006$ for the LCLC used in this work

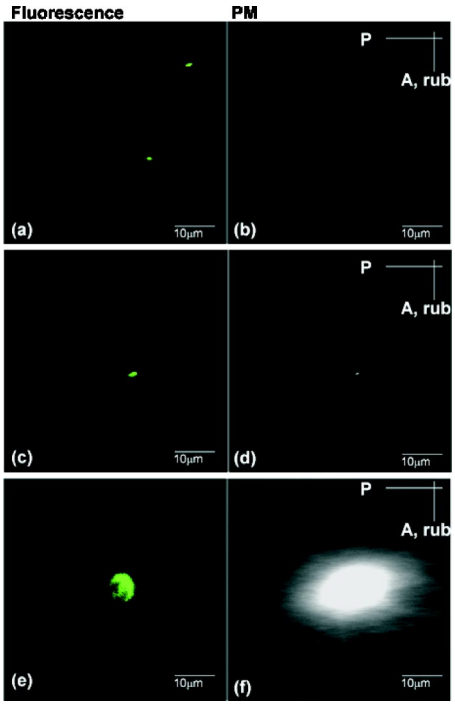

FIG. 2. (Color online) Effect of immune complex size on the director distortions. Two images in each row represent the same portion of the sample viewed either in fluorescence (left) or polarizing (right) mode. (a) Individual beads or their small complexes with $d<2$ μm cause (b) no detectable director distortions; (c) complexes with size $d\approx 2$ μm give rise to (d) minimal distortions; (e) large compexes, $d\approx 5$ μm, cause (f) significant director distortions over a scale much larger than d.

[17]. Thus when $|\Theta'|\lambda<1$, we can use the approximate expressions $q_j\approx\kappa\pm\kappa\delta\sqrt{1+\mu^2}$ and $\alpha_j\approx\frac{1}{2}\tan^{-1}\mu$ in Eq. (7) with accuracy better than 1%. Here $\kappa=\pi(n_e+n_o)/\lambda$ and $\mu=\Theta'/(\kappa\delta)$ coincides with the definition above. The effect of deviation of the light propagation direction from the normal on integrated transmitted intensity I_t, caused by distortions around a particle, is negligibly small. Thus,

$$I_t = I_0\int_R^\infty \rho d\rho\int_0^{2\pi} d\Phi|t|^2 \tag{8}$$

is expressed through the transmittance coefficient $t=\hat{\mathbf{P}}_\mathbf{A}\mathbf{S}^{-1}\mathbf{T}\mathbf{S}\hat{\mathbf{P}}_\mathbf{P}$, where $\hat{\mathbf{P}}_{P(A)}$ is the unit vector defining the orientation of the polarizer (analyzer), $\mathbf{T}$ is the 2×2 transmission matrix in the LC, so that $\tilde{A}_i(z_0+h)=T_{ij}\tilde{A}_j(z_0)$, where $\tilde{A}_i(z)=A_i(z)\exp\{i\Psi_i(z)\}$, and $\mathbf{S}$ is the matrix that determines the transformation between tangential components of the electric field and $\tilde{A}_j$ at the boundaries between LC and substrates. When the cell is viewed between two crossed polarizers, one of which is along $\hat{\mathbf{a}}$, then in the first perturbation order,

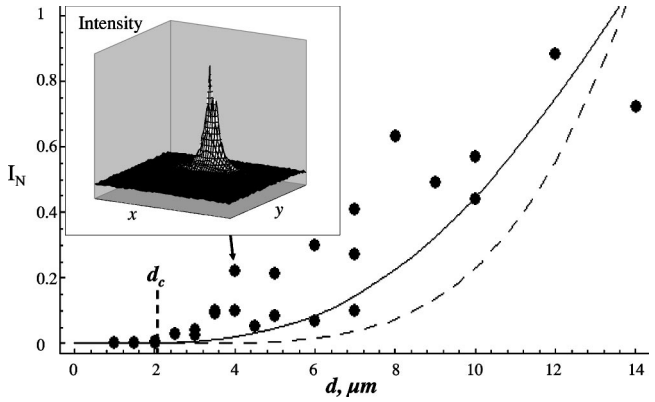

FIG. 3. Normalized light transmission, I_N, through a 15-μm-thick LCLC sample in the polarized light microscopy mode vs the average diameter of the immune complexes. Light transmission was determined in the polarizing microscope mode while the complex's size was determined in the fluorescent mode. The inset shows the signal intensity created by $d\approx 4$ μm complex over a 50×50 μm area of LCLC. The theoretical curves are calculated according to Eq. (11) with $|L|=5.65$ μm: the solid line corresponds to the strong anchoring, $\beta_0=$const, and the dashed line to the weak anchoring, in which case $\beta_0\propto d$, Eq. (3).

$$|t| = \left|\Theta_1-\Theta_2\exp\{i\overline{\Delta\Psi}\} + \frac{1}{L}\int_{z_0}^{z_0+h}\tan^{-1}\mu\sqrt{1+\mu^2}\exp\{i\Delta\Psi(z)\}dz\right|, \tag{9}$$

where $\Theta_{1(2)}$ is the angle between the perturbed $\hat{\mathbf{n}}$ and $\hat{\mathbf{a}}$ at the input (output) boundary.

If $h\gg R$, then $\Theta_{1,2}=0$ and

$$|t| = \left|\frac{2}{L}\int_0^\infty \tan^{-1}\mu\sqrt{1+\mu^2}\sin\Delta\Psi_0(z)dz\right|, \tag{10}$$

where $\Delta\Psi_0(z)=L^{-1}\int_0^z\sqrt{1+\mu^2}d\tilde{z}$. Expanding $|t|$ with respect to $c=\beta_0R^3L\sin 2\Phi/\rho^4$, one obtains $|t|=(c\nu^4/3)\mathcal{K}_2(\nu)$, where $\nu=\rho/L$ and $\mathcal{K}_i(\nu)$ is the modified Bessel function of the order i. Substituting $|t|$ in (8) we obtain the final expression

$$I_t = I_0\frac{\pi\beta_0^2R^8}{9L^6}\left\{\mathcal{K}_1\left(\frac{R}{L}\right)\mathcal{K}_3\left(\frac{R}{L}\right)-\mathcal{K}_2^2\left(\frac{R}{L}\right)\right\}. \tag{11}$$

The dependence $I_t(R)$ is steep: $I_t(R)\propto R^6$ for weak anchoring at the particle's surface and $I_t(R)\propto R^4$ for strong anchoring when β_0 is constant.

EXPERIMENT

Solutions of disodium cromoglycate (DSCG, Spectrum Chemical Manufacturing Corp.) in deionized water served as the nematic LCLC matrix to study the effects of immune complex formation. We used fluorescent-labeled (Dragon Green fluorochrome), antigen-coated (streptavidin) latex beads (Bangs Laboratories, Inc.), $d=0.56$ μm. An anti-streptavidin antibody (1.0 mg/mL; Rockland, Inc.) contained the a second fluorescent label. The beads (concentra-

tion 10^6-10^7 per mL) and the antibodies (0.01–1.0 mg/mL) were added to the LCLC so that the final concentration of DSCG in water was 13 wt %; it corresponds to the nematic phase of LCLC. The LCLC mixtures with beads only and antibodies only served as control samples. The glass plates coated with rubbed polyimide SE-7511 (Nissan Chemical) set the planar alignment of LCLC [10]. The samples were of thickness 8–30 μm and sealed.

The samples were evaluated 30 min after the preparation, under the microscope BX-50 Olympus, in two complementary modes: (1) fluorescence microscopy to identify the labelled beads and their complexes and to determine the size of complexes, Figs. 2(a), (c), (e); and (2) polarized light microscopy (of the same area of sample) to evaluate director distortions and corresponding light transmittance, Figs. 2(b), 2(d), and 2(f). The individual beads and antibodies in control samples and complexes with $d<2$ μm did not cause noticeable light transmission, Fig. 2(b). In contrast, complexes larger than $d_c \approx 2$ μm produced noticeable light transmission, Fig. 3, caused by director distortions over the area much larger than the complexes themselves [compare Figs. 2(e) and 2(f)]. In Fig. 3, the polarized microscopy mode was used to measure the transmittance of light (Kr laser $\lambda = 0.568$ μm) passing through a $H \times H = 50 \times 50$ μm area normalized as $I_N = (I_t - I_b)/(\bar{I}_b - I_b)$. Here I_t is the light intensity transmitted through the area with the complex, I_b is the light intensity transmitted through the uniform part of the same sample, and $\bar{I}_b$ is the transmittance through the same uniform area rotated by $\Theta_0 = 5^\circ$ with respect to the polarizer; $\bar{I}_b - I_b = I_0 H^2 \sin^2 2\Theta_0 \sin^2(h/2L) \approx 71$ μm^2. Thus I_N is normalized by the uniform bright field and reflects the relative amplitude (angle β) of director distortions.

The experimental and theoretical [Eq. (11) with $|L| = 5.65$ μm] dependencies $I_N(d)$ show a similar behavior. The solid line (strong anchoring, $\beta_0 = \text{const}$) fits the data better than the dashed line [weak anchoring, β_0 is determined by Eq. (4)]. The fitting coefficient for solid line is approximately four times larger that the value estimated from Eq. (11) with $\beta_0 = \pi/4$. The discrepancy is caused by a nonspherical shape of complexes and the finite h that results in $\Theta_{1,2} \neq 0$ and finite limits of integration in Eq. (9).

The steep dependence $I_N(d)$ allows one to introduce the critical size d_c, below which I_N can be considered as negligible; d_c depends on ξ, L, and h, Eqs. (3) and (8)–(11). In principle, d_c can be tuned (for example, by tuning the anchoring length ξ) in the range of 0.1–10 μm, which is the range of interest for microbiological applications. In such a case, microbes and antibodies, being individually too small to perturb $\hat{\mathbf{n}}$, will remain "invisible," while immune complexes will be amplified by distortions and brought into evidence by optical transmission. The biological selectivity of detection is guaranteed by the selectivity of antibody-antigen binding. The biosensor would function in real time as determined by formation of immune aggregates.

ACKNOWLEDGMENTS

The work was supported by NSF/ITIC Grant No. DMR-0346348, by MicroDiagnosis, Inc., and by the donation from Jessie Brown.

[1] V. K. Gupta, J. J. Skaife, T. B. Dubrovsky, and N. L. Abbott, Science **279**, 2077 (1998).
[2] C. J. Woolverton, G. D. Niehaus, K. J. Doane, O. Lavrentovich, S. P. Schmidt, and S. A. Signs, U.S. Patent No. 6,171,802 (2001).
[3] J. Fang, W. Ma, J. Selinger, and R. Shashidhar, Langmuir **19**, 2865 (2003).
[4] J. Hoogboom, J. Clerx, M. B. J. Otten, A. E. Rowan, T. Rasing, and R. J. M. Nolte, Chem. Commun. (Cambridge) **2003**, 2865 (2003).
[5] Y. Choi, Y. Lee, H. Kwon, and S. D. Lee, Mater. Sci. Eng., C **24**, 237 (2004).
[6] M. Kleman and O. D. Lavrentovich, *Soft Matter Physics: An Introduction* (Springer, New York, 2003), p. 638.
[7] Y.-Y. Luk, S. F. Campbell, N. L. Abbott, and C. J. Murphy, Liq. Cryst. **31**, 611 (2004).
[8] C. Woolverton, E. Gustely, L. Li, and O. D. Lavrentovich, Liq. Cryst. (to be published).
[9] J. Lydon, Curr. Opin. Colloid Interface Sci. **3**, 458 (1998); **8**, 480 (2004).
[10] O. D. Lavrentovich and T. Ishikawa, US Patent No. 6,411,354 (2002).
[11] B. Eggins, *Biosensors: An Introduction* (Wiley, Chichester, 1997), p. 212.
[12] O. V. Kuksenok, R. W. Ruhwandl, S. V. Shiyanovskii, and E. M. Terentjev, Phys. Rev. E **54**, 5198 (1996).
[13] P. Poulin, H. Stark, T. C. Lubensky, and D. Weitz, Science **275**, 1770 (1997).
[14] H. Stark, Phys. Rep. **351**, 387 (2001).
[15] P. Allia, C. Oldano, and L. Trossi, Mol. Cryst. Liq. Cryst. **143**, 17 (1987).
[16] S. Faetti and G. C. Mutinati, Phys. Rev. E **68**, 026601 (2003).
[17] Yu. A. Nastishin *et al.* (unpublished).